CALORIMETRIC STUDY OF PHASE TRANSITIONS OF $Ag_8SiS_6(Se_6)$ COMPOUNDS

S.R. Aslanly[1], L.F. Mashadiyeva[2*], Z.T. Hasanova[3], A.A. Gasanov[4], M.B. Babanly[2,5]

[1]Institute of Ecology and Natural Resources, G.Aliyev Ave., 419, AZ-2000, Ganja, Azerbaijan
[2]Institute of Catalysis and Inorganic Chemistry, G.Javid Ave., 113, AZ-1143, Baku, Azerbaijan
[3]Baku State University, Z.Khalilov, 23, AZ-1148, Baku, Azerbaijan
[4]Azerbaijan State Oil and Industry University, 34 Azadliq Avenue, AZ-1010, Baku, Azerbaijan
[5]Azerbaijan State University of Economics Baku, Azerbaijan
[*]e-mail: leylafm76@gmail.com

Received 27.02.2025
Accepted 20.05.2025

Abstract: *Polymorphic transitions in the Ag_8SiS_6 and Ag_8SiSe_6 compounds were studied by differential scanning calorimetry (DSC). Two samples of each compound with different sample weights in the range from 20 to 50 mg were selected for the studies, for which three DSC heating curves were recorded. Based on the DSC curves, the temperatures and enthalpies of phase transitions of the studied compounds from the low-temperature rhombic modification to the high-temperature cubic modification were determined. The data obtained on all DSC heating curves for each sample did not exceed 2%. The entropies of these transitions (ΔSp.t.) were calculated from the values of heats and temperatures. It was shown that the values of ΔSp.t. both compounds have anomalously high values, which can be explained by the complete delocalization of silver ions in the cation sublattice during the transition from low-temperature modifications to high-temperature cubic ion-conducting phases.*

Keywords: *argyrodite, phase transition, enthalpy and entropy of phase transformation, thermodynamic functions, differential scanning calorimetry*
DOI: 10.65382/2221-8688-2026-1-104-110

Introduction

The mineral argyrodite (Ag_8GeS_6) and its analogs with the general formula $A_8B^{IV}X_6$ (where A is Li, Cu, Ag; BIV is Si, Ge, Sn; X is S, Se, Te) attract attention as polyfunctional materials and are the object of study of many research groups [1-6]. All these compounds, despite the diversity of composition, demonstrate anomalously low lattice thermal conductivity, almost independent of temperature, which indicates their glass-like thermal conductivity. On the other hand, the rigid anionic framework of the crystal lattice provides electron transport as in conventional semiconductors. For this reason, compounds of the argyrodite family are considered good matrix compounds for the development of high-performance thermoelectric materials by separately tuning the electrical properties and thermal conductivity [7-13].

Most compounds of the argyrodite family have phase transitions at relatively low temperatures. High-temperature phases, as a rule, crystallize in a cubic structure, and low-temperature modifications have lower symmetry. Analysis of the literature shows that most high-temperature phases of these compounds, due to the features of the crystal structure, have mixed electron-ion conductivity and demonstrate high values of cation conductivity for solids due to the high mobility of copper (or silver) ions [14-20]. This makes them promising materials for ion-selective electrodes, solid electrolytes in the development of various types of electric batteries, sensors, etc.

The aim of this study was to determine the thermodynamic functions of phase transitions of Ag_8SiS_6 and Ag_8SiSe_6 compounds using differential scanning calorimetry (DSC). This method is considered to be one of the most advanced, sensitive and accurate methods for measuring thermal effects. Previously, in [21-26], calorimetric studies of phase transitions of a number of compounds of the argyrodite family based on copper and silver were carried out and

the values of their thermodynamic functions were determined.

The nature of melting and the crystal structures of the objects of our study have been studied in detail in a number of works. The Ag_8SiS_6 compound melts congruently at 1232 K [27], 1213 K [28] or 1225 K [29] and has a phase transition at 507 K [28] or 510 K [29]. The high-temperature modification crystallizes in a cubic lattice (Sp. gr. *F-43m*; a = 1.063 nm [30]), and the low-temperature modification has an orthorhombic lattice (Sp. gr. $Pmn2_1$; a = 1.5024 nm, b = 0.7428 nm, c = 1.0533 nm [30] or a = 1.5043 nm, b = 0.7452 nm, c = 1.0565 nm [31]).

Ag_8SiSe_6 melts congruently. Various works give very different values for the melting point of this compound. Thus, according to data of [28, 32], it melts at 1203 K. Other works give the following data: 1258 K [29], 1268 K [33]. According to more recent data [34], this compound melts at 1278 K and undergoes polymorphic transformations at 315 and 354 K.

According to the available literature data, the Ag_8SiSe_6 compound has at least 3 crystalline modifications. However, different authors provide different data on the modifications of this compound. Taking into account the discrepancies in the literature data on the melting point and crystallographic data, a repeated study of this compound was undertaken in [34]. According to this work, the high-temperature (HT) modification of this compound, like all other compounds of the argyrodite family, crystallizes in a face-centered cubic structure (Sp. gr. *F-43m*; a = 1.0891 nm), and the intermediate modification (IT) has a cubic structure with Sp. gr. $P4_232$ (a = 1.0965 nm) [28]. The IT- Ag_8SiSe_6 modification is characterized by partial localization of silver ions [16]. The data on the structure of the low-temperature modification (LT- Ag_8SiSe_6) are contradictory. According to [28, 32], LT-Ag_8SiSe_6 has a tetragonal structure (Sp. gr. *I-4m2*; a = 0.7706, b = 1.10141 nm). However, the authors of [12] note that the powder diffraction pattern of LT- Ag_8SiSe_6 is poorly indexed in this structure. According to their results, the diffraction pattern contains 2 series of reflection lines, and most of the peaks are indexed in the rhombic structure (Sp. gr. $Pmn2_1$).

Experimental part

Synthesis. The Ag_8SiS_6 and Ag_8SiSe_6 compounds were synthesized by direct fusion of high-purity (≥99.999%) elemental components from Evochem Advanced Materials GMBH (Germany). The synthesis was carried out in evacuated (~10^{-2} Pa) and sealed quartz ampoules in a two-zone mode. The synthesis temperature mode for each compound was selected taking into account their melting and phase transition temperatures. The ampoule with the reaction mixture was heated in an inclined tubular furnace to a temperature ~50° higher than the melting point of the synthesized compound ("hot" zone). To control the vapor pressure of sulfur or selenium and prevent the ampoule from exploding, a part of the ampoule (~8 cm) outside the furnace was cooled with water ("cold" zone). To accelerate the interaction, the ampoule was rotated around its longitudinal axis and subjected to vibration. After the interaction of the main mass of sulfur or selenium, the ampoule was completely introduced into the furnace and held in the hot zone for one hour. Then the ampoule was cooled (very slowly in the region of the temperature of the polymorphic transformation), and then subjected to thermal annealing slightly below these temperatures for 10-15 hours. This was done in order to ensure a complete transition of the high-temperature phase to the low-temperature one, in order to minimize the error in calculating the enthalpy.

The synthesized compounds were identified by X-ray Diffraction technique (XRD). XRD of the samples was carried out on a D8 ADVANCE powder diffractometer from Bruker (Germany) with $CuK\alpha_1$ radiation. The XRD results confirmed the single-phase nature of the synthesized compounds and showed that the diffraction patterns of the samples slowly cooled after synthesis completely coincide with the X-ray data of low-temperature rhombic modifications [12, 30, 31].

Experimental procedure. The temperatures and heats of phase transitions of the studied compounds were determined by the DSC method on a differential scanning calorimeter DSC400 from Linseis (Germany). As is known, in the DSC method, the enthalpy of phase

transition is determined through the heat flow - the derivative of heat with respect to time [35, 36].

The measurements were carried out using the Linseis TA V 2.3.1 program. The calorimeter was preliminarily calibrated. Our studies were carried out at low temperatures, therefore, relatively low-melting metals were used as standards for calorimeter calibration: indium, tin, bismuth and zinc, provided by Linseis for this purpose with the appropriate certificates. The temperature mode of calibration of each of the substances was selected in accordance with the recommendations given in the manual for the use of the calorimeter.

DSC of the compounds and standards was performed using an aluminum crucible with a lid. Before the measurement, solid polycrystalline samples of the compounds under study were preliminarily ground to a powder state in order to ensure the maximum possible contact area between the sample and the crucible bottom. The samples were weighed using precise (1st accuracy class according to GOST) electronic analytical scales from Radwag (Poland) of the AS220 series with a range from 1 mg to 220 g and a measurement accuracy of 0.01/0.1 mg. The dynamic temperature heating mode during DSC was selected taking into account the phase transition temperature of the compound under study. The heating rate was 3 °/min. The measurements were performed in an argon flow. The DSC study technique is described in more detail in [21, 23].

Results and discussion

We recorded the DSC heating curves for the compounds Ag_8SiS_6 and Ag_8SiSe_6. For each compound, two samples with masses varying from 20 to 50 mg were selected, for which three DSC heating curves were recorded. As a result, six DSC curves were recorded for each compound, which were processed using the Linseis TA Evaluation V2.3.1 software. As a result, the values of the phase transition enthalpy for 1 mole of the substance, as well as the temperatures of the beginning and end of the peak were obtained. These values for each sample almost coincided on all six DSC curves and differed by no more than 2%. According to [35, 36], in such cases the error in determining the thermal effects does not exceed ±4%.

Let us consider the DSC study and the calculation process of the thermodynamic functions of the phase transition for the Ag_8SiS_6 compound. We selected two weighed portions of this compound with masses of 28.93 and 44.51 mg. Taking into account the phase transition temperature of the Ag_8SiS_6 compound [28, 29], the DSC study was carried out in the dynamic heating mode from room temperature to 535 K. The DSC heating curve for the Ag_8SiS_6 sample with a mass of 44.51 mg is shown in Fig. 1. From these six DSC curves, the following average values of the phase transition enthalpies were obtained: $\Delta H_{p.t.}$ = 6.49 kJ/mol (28.93 mg) and $\Delta H_{p.t.}$ = 6.47 kJ/mol (44.51 mg).

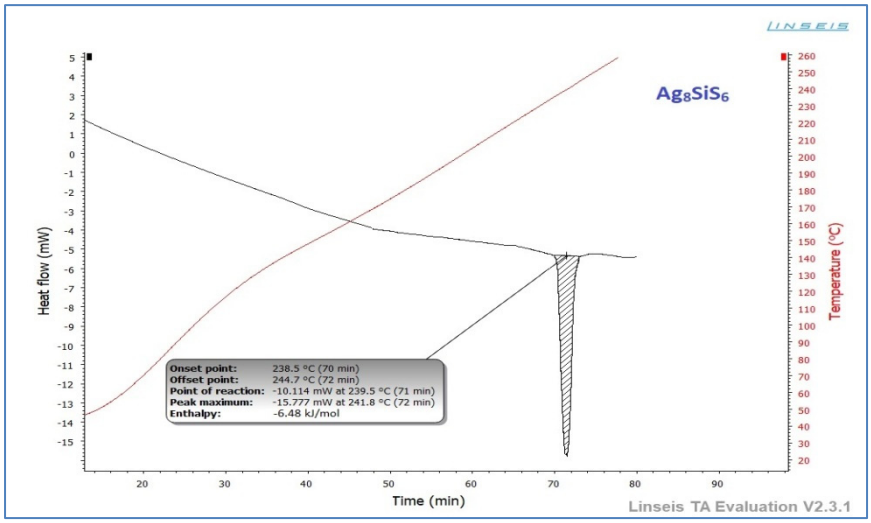

Fig. 1. DSC heating curve of the Ag_8SiS_6 compound with a sample weight of 44.51 mg

The average value of these quantities was taken as the final value of ΔHp.t. for the Ag_8SiS_6 compound (Table).

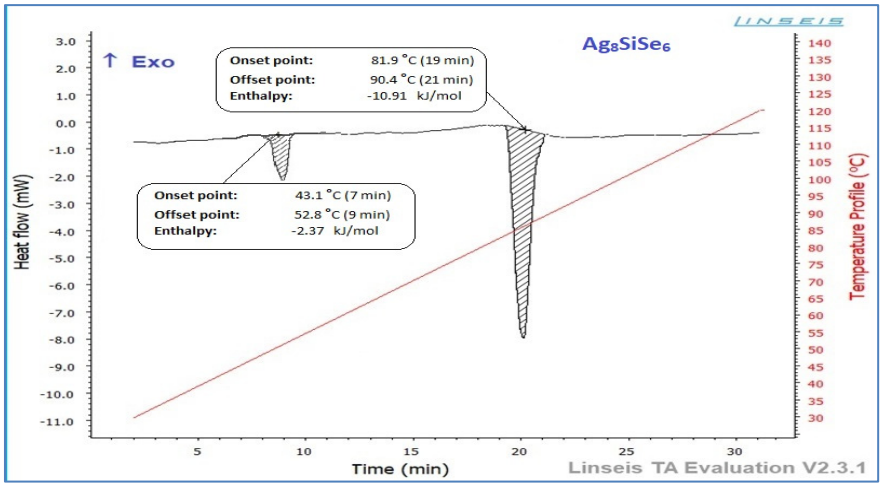

Fig. 2. DSC heating curve of the Ag_8SiSe_6 compound with a sample weight of 36.68 mg

Table. Thermodynamic data of phase transitions of Ag_8SiS_6 and Ag_8SiSe_6 compounds

Compound	Phase transition temperature, K	$\Delta H_{p.t.}$, кJ/mole	$\Delta S_{p.t.}$, J/(mole·K)
Ag_8SiS_6	512	6.48±0.26	12.66±0.51
Ag_8SiSe_6	316	2.34±0.09	7.41±0.30
	354	10.91±0.44	30.82±1.23

In a similar manner, the temperatures and average enthalpy values were determined for two phase transitions of the Ag8SiSe6 compound (Fig. 2, Table). Using the obtained values of enthalpies and temperatures (Tonset) of the phase transitions, the entropies of the phase transitions were calculated (table) using the formula:

$$\Delta S_{p.t.} = \Delta H_{p.t.}/T_{p.t.}$$

It is evident from the table that the entropy value of the phase transition of the Ag_8SiSe_6 compound at 316 K is significantly lower compared to the transition at 354 K. Apparently, this is due to the fact that during the transition from the low-temperature modification to the medium-temperature one, only some of the silver ions acquire mobility [16]. During the transition from the medium-temperature phase to the high-temperature cubic one, complete delocalization of silver ions is observed, which is accompanied by a high value of the phase transition entropy. On the other hand, the entropy value of the phase transition of selenide (Ag_8SiSe_6) at 354 K is significantly higher compared to sulfide (Ag_8SiS_6). This regularity was also observed for other argyrodite compounds based on silver [21]. This is probably due to the fact that silver ions in the cubic lattice of selenides are more disordered compared to sulfides.

A comparison of the table and the results of our previous works [21-26] with the literature data on the thermodynamic functions of phase transitions of a number of chalcogenides of other types [37] show that the values of such functions for our objects of study are quite high compared to the values of the thermodynamic functions of first-order phase transitions. Obviously, this is a consequence of the fact that during the polymorphic transformation of argyrodite compounds, more significant structural changes occur, accompanied by delocalization of silver cations.

Conclusion

We have presented new data on the thermodynamic functions of phase transitions of Ag_8SiS_6 and Ag_8SiSe_6 compounds obtained by the DSC method. It is shown that the entropies of phase transitions of both compounds have anomalously high values, which can be explained by strong disordering in the cation sublattice during the transition from low-temperature modifications to high-temperature cubic ion-conducting phases, which is accompanied by complete delocalization of silver ions.

References

1. Tee S.Y., Ponsford D., Lay C.L., Wang X., Wang X., Neo D.C.J., Wu T., Thitsartarn W., Yeo J.C.C., Guan G., Lee T.-C., Han M-Y. Thermoelectric Silver-Based Chalcogenides. *Advanced Science.* 2022, **Vol. 9(36),** p. 1-35. https://doi.org/10.1002/advs.202204624
2. Lin S., Li W., Pei Y. Thermally insulative thermoelectric argyrodites. *Materials Today*. 2021, **Vol. 48**, p. 198-213. https://doi.org/10.1016/j.mattod.2021.01.007
3. Semkiv I., Ilchuk H., Pawlowski M., Kusnezh V. Ag_8SnSe_6 argyrodite synthesis and optical properties. *Opto-Electronics Review.* 2017, **Vol. 25(1)**, p. 37–40. https://doi.org/10.1016/j.opelre.2017.04.002
4. Semkiv H., Ilchuk N., Kashuba A. Photoluminescence of Ag_8SnSe_6 argyrodite. *Low Temperature Physics*. 2022, **Vol. 48**, p. 12-15. https://doi.org/10.1063/10.0008957
5. Li Z., Liu C., Zhang X., Zhang Z., Guo W., Shen L., Long Y. An easily prepared Ag_8GeS_6 nanocrystal and its role on the performance enhancement of polymer solar cells. *Organic Electronics*. 2017, **Vol. 45**, p. 247–255. https://doi.org/10.1016/j.orgel.2017.03.029
6. Jin Z., Xiong Y., Zhao K., Dong H., Ren Q., Huang H., Shi X. Abnormal thermal conduction in argyrodite-type Ag_9FeS_6-Te materials. *Materials Today Physics*. 2021, **Vol. 19**, p.100410. https://doi.org/10.1016/j.mtphys.2021.100410
7. Shen X., Yang C.-C., Liu Y., Wang G., Tan H. High Temperature Structural and Thermoelectric study of Argyrodite Ag_8GeSe_6. *ACS Applied Materials & Interfaces.* 2019, **Vol. 11(2)**, p. 2168-2176. https://doi.org/10.1021/acsami.8b19819
8. Jin M., Lin S., Li W., Chen Z., Li R., Wang X., Pei Y. Fabrication and thermoelectric properties of single-crystal argyrodite Ag_8SnSe_6. *Chemistry of Materials*, 2019, **Vol. 31(7)**, p. 2603-2610. https://doi.org/10.1021/acs.chemmater.9b00393
9. Wang B., Li S., Luo Y., Yang J., Ye H., Liu Y., Jiang Q. A new thermoelectric Ag8SiSe6 argyrodite for room temperature application: sensitivity of thermoelectric performance to cooling conditions. *Materials Advances*, 2024, **Vol. 5**, p. 3735–3741. https://doi.org/10.1039/d3ma01190a
10. Yang C., Luo Y., Li X., Cui J. N-type thermoelectric Ag_8SnSe_6 with extremely low lattice thermal conductivity by replacing Ag with Cu, *RSC Advances.* 2021, **Vol. 11(6),** p. 3732-3739. https://doi.org/10.1039/D0RA10454J
11. Namiki H., Yahisa D., Kobayashi M., Shono A., Hayashi H. Enhancement and manipulation of the thermoelectric properties of n-type argyrodite Ag_8SnSe_6 with ultralow thermal conductivity by controlling the carrier concentration through Ta doping. *AIP Advances.* 2021, **Vol. 11(7)**, 075125. https://doi.org/10.1063/5.0056533
12. Jiang Q., Li S., Luo Y., Xin J., Li S., Li W., Yang J. Ecofriendly Highly Robust Ag_8SiSe_6-Based Thermoelectric Composites with Excellent Performance Near Room Temperature. *ACS Applied Materials & Interfaces*, 2020, **Vol. 12(49),** p. 54653–54661. https://doi.org/10.1021/acsami.0c15877
13. Fan Y., Wang G., Wang R., Zhang B., Shen X., Jiang P., Zhang X., Gu H.-S., Lu X., Zhou X.-Y. Enhanced thermoelectric properties of p-type argyrodites Cu_8GeS_6 through Cu vacancy. *Journal of*

Alloys and Compounds. 2020, **Vol. 822**, p. 153665. https://doi.org/10.1016/j.jallcom.2020.153665

14. Ayoola O., Buldum A., Farhad S., Ojo S. A Review on the Molecular Modeling of Argyrodite Electrolytes for All-Solid-State Lithium Batteries. *Energies*, 2022, **Vol**. **15**, p. 7288. https://doi.org/10.3390/en15197288
15. Sardarly R.M., Babanly M.B., AliyevaN.A., Mashadiyeva L.F., Mamadov R.A., Ashirov G.M., Saddinova A.A., Damirova S.Z. Obtaining and measuring impedance characteristics of the Ag_8SiSe_6 compound. *East European Journal of Physics*, 2025, **Vol. 1**, p. 233-239. https://doi.org/10.26565/2312-4334-2025-1-24
16. Heep B.K., Weldert K.S., Krysiak Y., Day T.W., Zeier W.G., Kolb U., Snyder G.J., Tremel W. High electron mobility and disorder induced by silver ion migration lead to good thermoelectric performance in the argyrodite Ag_8SiSe_6. *Chemistry of Materials.* 2017, **Vol. 29(11)**, p. 4833−4839. https://doi.org/10.1021/acs.chemmater.7b00767
17. Sardarly R.M., Ashirov G.M., Mashadiyeva L.F., Aliyeva N.A., Salmanov F.T., Agayev R.Sh., Mamedov R.A., Babanly M.B. Ionic conductivity of the Ag_8GeSe_6 compound. *Mod. Phys. Lett. B,* 2023, **Vol. 36(32n33),** 2250171. https://doi.org/10.1142/S0217984922501718
18. Lin Y., Fang S., Su D., Brinkman K.S. Enhancing grain boundary ionic conductivity in mixed ionic–electronic conductors. *Nature Communications.* 2015, **Vol**. **6(1),** p. 1-9. https://doi.org/10.1038/ncomms7824
19. Liu H., Shi X., Xu F., Zhang L., Zhang W., Chen L., Li Q., Uher C., Day T., Snyder G.J. Copper ion liquid-like thermoelectrics. *Nature Materials*. 2012, **Vol. 11(5)**, p. 422–425. https://doi.org/10.1038/nmat3273
20. Pogodin A., Filep M., Studenyak V., Symkanych O., Stercho I., Izai Y.V., Kokhan O., Kúš P. Influence of crystal structure disordering on ionic conductivity of $Ag_{7+x}(P_{1-x}Ge_x)S_6$ single crystals. *Journal of Alloys and Compounds*. 2022, **Vol**. **926,** 166873. https://doi.org/10.1016/j.jallcom.2022.166873
21. Bayramova U.R., Poladova A.N., Mashadiyeva L.F., Babanly M.B. Calorimetric determination of phase transitions of Ag_8BX_6 (B=Ge, Sn; X=S, Se) compounds. *Condensed Matter and Interphases*. 2022, **Vol**. **24(2)**, p. 187-195. https://doi.org/10.17308/kcmf.2022.24/9258
22. Bayramova U.R. Determination of the thermodynamic functions of the phase transition of the Cu_8SiSe_6 compound by the DSC method. *Chemical Problems*, 2022, **Vol**. **20(2)**, p. 116-121. https://doi.org/10.32737/2221-8688-2022-2-116-121
23. Bayramova U.R., Babanly K.N., Ahmadov E.I., Mashadiyeva L.F., Babanly M.B. Phase equilibria in the Cu_2S-Cu_8SiS_6-Cu_8GeS_6 system and thermodynamic functions of phase transitions of the $Cu_8Si_{(1-X)}Ge_XS_6$ argyrodite phases. *Journal of Phase Equilibria and Diffusion*. 2023, **Vol**. **44**, p. 509-519. https://doi.org/10.1007/s11669-023-01054-y
24. Bayramova U.R., Ahmadov E.I., Babanly D.M., Mashadiyeva L.F., Babanly M.B. Calorimetric study of phase transition of Cu_8GeSe_6 and comparison with other argyrodite family compounds. *Chemical Problems*, 2023, **Vol. 4(21)**, p. 396-403. https://doi.org/10.32737/2221-8688-2023-4-396-403
25. Babanly M.B., Yusibov Y.A., Imamaliyeva S.Z., Babanly D.M., Alverdiyev I.J. Phase Diagrams in the Development of the Argyrodite Family Compounds and Solid Solutions Based on Them. *Journal of Phase Equilibria Diffusion*. 2024, **Vol. 45**, p. 228–255. https://doi.org/10.1007/s11669-024-01088-w
26. Babanly M.B., Mashadiyeva L.F., Imamaliyeva S.Z., Tagiev D.B., Babanly D.M., Yusibov Yu.A. Thermodynamic properties of complex copper chalcogenides. *Chemical Problems*. 2024, **Vol**. **22(3)**, p. 243-280. https://doi.org/0.32737/2221-8688-2024-3-243-280

27. Cambi L, Elli M. Sui sulfogermanati: argirodite sintetica. *Atti della Academia Nazionale dei Lincei, Rendiconti, Classe di Scienze Fisiche, Mathematiche e Naturali.* 1961, **Vol**. **30**, p. 11-15.
28. Gorochov O., Flahaut J. Les composes Ag_8MX_6 avec M = Si, Ge, Sn et X= S, Se, Te. *Comptes rendus de l'Académie des Sciences.* 1967, **Vol. 264**, p. 2153-2155 [in French]
29. Venkatraman M., Blachnik R., Schlieper A. The phase diagrams of M_2X-SiX_2 (M is Cu, Ag; X is S, Se). *Thermochimia Acta*. 1995, **Vol. 249**, p. 13-20. https://doi.org/10.1016/0040-6031(95)90666-5
30. Gorochov O. Les composes Ag_8MX_6 (M = Si, Ge, Sn et X = S, Se, Te). *Bull. Soc. Chim. Fr.* 1968, **Vol. 6**, p. 2263-2275 [in French.]
31. Krebs B., Mandt J. Zur Kenntnis des Argyrodit-Strukturtyps: die Kristallstruktur von Ag_8SiS_6. *Zeitscrift für Naturforschung B*. 1977, **Vol**. **32**, p. 373-379. https://doi.org/10.1515/znb-1977-0404
32. Hofmann A.M. S*ilver-Selenium-Silicon. Ternary Alloys*. *VCH 2*, 1988, p. 559–560.
33. Piskach L.V., Parasyuk O.V., Olekseyuk I.D., Romanyuk Y.E., Volkov S.V. *Journal of Alloys and Compounds*. 2006, **Vol. 421**, p. 98–104. doi: 10.1016/j.jallcom.2005.11.056
34. Amiraslanova A.J., Babanly K.N., Imamaliyeva S.Z., Alverdiyev I.J., Yusibov Yu.A., Babanly M.B. *Applied Chemical Engineering*. 2023, **Vol**. **6(2)**, p. 1-9. doi: 10.24294/ace.v6i2.2162
35. Hohne G.W.H., Hemminger W.F. Flammersheim H.J. *Differential Scanning Calorimetry*. (Second Edition), Berlin: Springer. 2003. 298 p. https://doi.org/10.1007/978-3-662-06710-9
36. Menczel J., Grebowicz J. *The Handbook of Differential Scanning Calorimetry: Techniques and Low Molecular Mass Materials*. Elsevier Science. 2022. 858 p.
37. *Physical and chemical properties of semiconductor substances [Fiziko-khimicheskiye svoystva poluprovodnikovikh veshestv]*. Handbook. Ed. Novoselova A.V., Lazereva V.B. Moscow: Nauka Publisher. 1976. 339 p. (In Russ.)